ISSN 1541-308X, Physics of Wave Phenomena, 2008, Vol. 16, No. 4, pp. 300–304. © Allerton Press, Inc., 2008.

SURFACE ACOUSTIC WAVES

Localization of Rayleigh Waves in Microfluidic Channels with Quadratic Profile

A. V. Zyryanova* **and V. G. Mozhaev****

Lomonosov Moscow State University, Leninskie Gory 1, Moscow 119991, Russia

Received July 29, 2008

Abstract—Localization of Rayleigh waves due to mechanical loading of the substrate surface by a liquid layer with quadratic thickness variation in the transverse direction was theoretically studied. Under conditions typical of acoustic biochips, strong localization of the wave field was revealed. This makes it possible to calculate the lowest waveguide modes of the microfluidic channel, neglecting its finite width.

PACS numbers : 43.35.+d, 43.35.Pt, 46.40.Cd, 68.35.Iv, 68.60.Bs
DOI: 10.3103/S1541308X08040079

Recently, surface acoustic waves (SAWs) at ultrasonic frequencies propagating in piezoelectric substrates have found unusual new and promising applications related to their use as a driving force in microfluidic processors of acoustic biochips [1]. These devices are intended for automated and prompt chemical and biological analyses of solutions in the form of microdrops with volumes of the order of micro- and nanoliters and for microsynthesis of required biological or chemical solutions. In such devices, SAWs can be used to perform various functions such as transport of drops, their controllable splitting into smaller drops, and enhancement of liquid mixing in drops due to acoustic radiation forces. It is expected that the development of efficient devices of this type can cause radical improvement and extended functionality of hardware of modern medicine, pharmacology, molecular biology, micro- and nanochemistry.

Previously, to achieve directed drop motion over piezoelectric crystalline substrates, it was proposed to use elements such as guide rails shaped as thin strips made of a material with better wettability than that of the substrate surface [1]. Such guide strips can have a significant effect not only on drops, but also on the spatial distribution of acoustic fields, leading, in particular, to their localization and waveguiding. At the same time, localization of acoustic waves is also possible due to the effect on them of the drop itself, in particular, when the drop forms an elongated microfluidic channel. It should be emphasized that information on the spatial distribution of acoustic fields in microfluidic processors of acoustic biochips is of fundamental importance for correct analysis of their functioning, since the efficiency of these devices is directly controlled by the amplitude of driving acoustic waves.

The goal of this paper is to theoretically study Rayleigh SAW localization when the substrate surface is loaded by a thin liquid layer with quadratic variation in the thickness in the transverse direction. The geometry of the problem is shown in Fig. 1. It is assumed that liquid is placed on the surface of Y-cut piezoelectric substrate, in which Rayleigh surface waves excited by interdigital transducers (IDTs) travel along the Z axis. Two types of surface loading, i.e., an elongated (quasi-two-dimensional) drop and a microfluidic cell shaped as a cylinder segment, are possible within this study. The former loading type is implemented when a drop spreads over the substrate exposed to surface waves [2]. The role of walls of the microfluidic channel is played by capillary forces. The latter loading type can be implemented by forming extended microtrenches on the surface (e.g., by selective etching). For thin liquid layers, the difference between these loading types is negligible, and the general solution that can be applied to both cases is presented below.

In acoustic microfluidic processors, various ratios of channel sizes to acoustic wavelengths can be implemented. Let us first consider the case of a thin liquid layer. The expression for a relative perturbation of the wavenumber $\Delta k/k_0$ for Rayleigh-type SAWs propagating in anisotropic piezoelectric substrates loaded by a thin plane-parallel isotropic elastic solid layer of thickness h is given in [3]. From this expression, assuming the layer shear modulus equal to zero,

*E-mail: annazyr@mail.ru
**E-mail: vgmozhaev@mail.ru

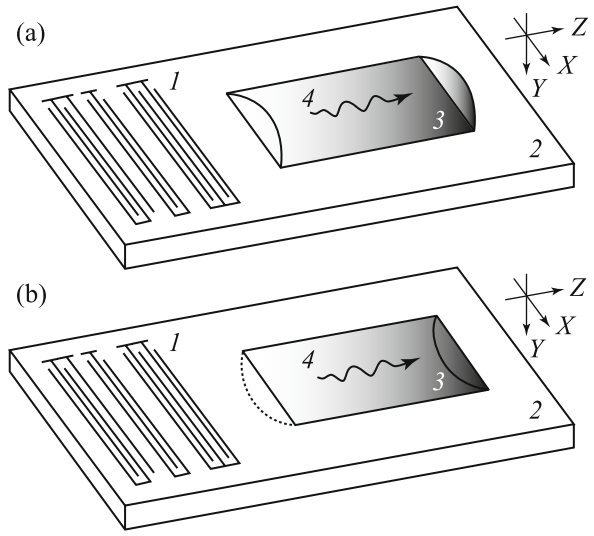

Fig. 1. Propagation of Rayleigh surface acoustic waves under a liquid layer with a quadratic profile: (a) substrate with elongated drop, (b) substrate with microfluidic cell; (*1*) interdigital transducers, (*2*) substrate, (*3*) liquid layer, and (*4*) Rayleigh waves.

the result for a nonviscous liquid layer is given by

$$\frac{\Delta k}{k_0} = Ah, \quad A = \frac{v_0 \rho_{\text{liq}}}{4}\left(\frac{|V_x|^2}{P} + \frac{|V_y|^2}{P} + \frac{|V_z|^2}{P}\right), \tag{1}$$

where k_0 and v_0 are, respectively, the wavenumber and phase velocity of Rayleigh waves on the free surface, ρ_{liq} is the liquid density, V_x, V_y, V_z, and P are, respectively, the components of the particle velocity and power flow per unit width along X in Rayleigh waves. The numerical values of these parameters or their ratios for a number of widely used substrate materials are given in [3]. All parameters entering the coefficient A in formula (1) are positive. From this it follows that the surface loading of both isotropic and anisotropic piezoelectric solids by a nonviscous liquid layer always leads to a decrease in the SAW velocity independently of a substrate material. Such a conclusion is consistent with the results of particular numerical calculations presented in [4–6]. This conclusion contradicts the incorrect one [7] about an increase in the velocity of the lowest mode of Rayleigh waves as the liquid layer thickness increases from zero (see the results of the later study [6]).

If the layer thickness varies slowly with distance, i.e., these variations are small at distances of the order of the wavelength, formula (1) can also be used to calculate the local wavenumber of Rayleigh waves under a variable-thickness layer. We further approximate the layer thickness variations across the channel by the parabolic dependence $h = h_0(1 - \beta x^2)$. Here x is the distance from the symmetry axis of the channel, h_0 is the maximum layer thickness at the channel center (at $x = 0$), and β is the coefficient defining the layer thickness variation rate with x. The relative channel width N expressed in terms of the Rayleigh wavelength λ_{R} at such a channel quadratic profile is given by $N = 2/(\lambda_{\text{R}}\sqrt{\beta})$. The channel parameters are considered to be unchanged in the direction of acoustic wave propagation.

To describe the spatial distribution of localized fields for time-harmonic (monochromatic) Rayleigh waves in microfluidic channels, we use the model scalar wave equation

$$\Delta_\perp \psi + k^2 \psi = 0, \tag{2}$$

where $\Delta_\perp = \partial^2/\partial x^2 + \partial^2/\partial z^2$ and k is the wavenumber of Rayleigh waves, which is further considered to be perturbed due to the presence of the layer, i.e., $k = k_0 + \Delta k$. Such an equation was strictly derived in [8] for one of the potentials ψ of displacement in three-dimensional Rayleigh waves in a homogeneous isotropic medium with free boundary. Three-dimensional waves are understood as waves whose field varies both with depth and along two other horizontal coordinates. Such a scalar wave model is used to simplify an analysis of complex waveguide problems for surface acoustic waves, including the case of inhomogeneous media with smoothly varying properties [9].

Substitution of the above expressions into Eq. (2) using the approximate relation $k^2 \approx k_0^2 + 2k_0\Delta k$ and the search for the solution in the form $\psi = \psi(x) \times \exp(ik_z z)$ reduce (2) to the Schrödinger equation for the linear harmonic oscillator:

$$\frac{d^2\psi(x)}{dx^2} + (p - \alpha^2 x^2)\,\psi(x) = 0, \tag{3}$$

where

$$p = k_0^2 - k_z^2 + 2k_0^2(\Delta k/k_0)_{\max},$$
$$\alpha^2 = 2k_0^2\beta(\Delta k/k_0)_{\max},$$
$$(\Delta k/k_0)_{\max} = Ah_0.$$

Equation (3) has the known exact solution describing the spatial distribution of waveguide modes

$$\psi_n = C_n \exp\left(-\frac{\xi^2}{2}\right) H_n(\xi) \exp(ik_z^n z),$$

where $H_n(\xi)$ are the Hermite polynomials of the nth degree ($n = 0, 1, 2, \ldots$), $\xi = \sqrt{\alpha}x$, C_n are arbitrary amplitude constants, and $p = (1 + 2n)\alpha$. The last condition determines the value of the wavenumber k_z for a mode with a given number n.

Due to the symmetry of IDTs used to excite SAWs, of most interest are the lowest symmetric modes, first of all, the zero mode ($n = 0$) with the pure Gaussian transverse distribution of the wave field. An

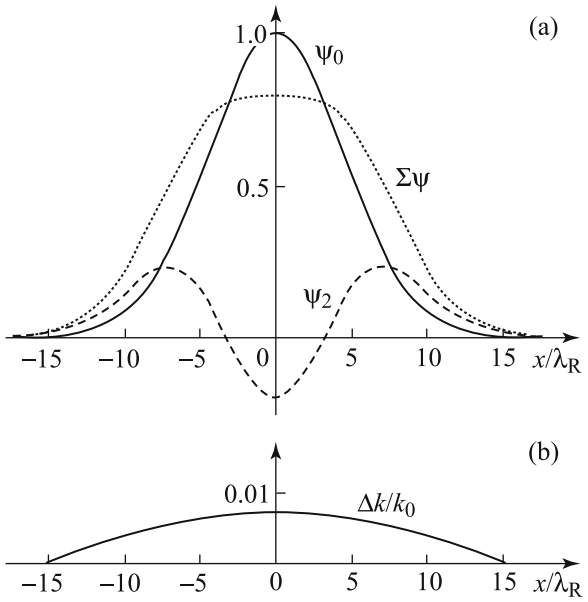

Fig. 2. Transverse distributions of wave characteristics in the microfluidic channel with a width of $30\lambda_R$: (a) fields of the zero and second Rayleigh waveguide modes and their sum and (b) the local wavenumber perturbation $\Delta k/k_0$ of Rayleigh waves.

example of calculating the field distribution of the two lowest symmetric modes ($n = 0, 2$) across the microfluidic channel whose width equal to 30 Rayleigh wavelengths on the Y-cut of $LiNbO_3$ substrate at $k_0h_0 = 0.2$ and wave propagation along the Z axis at frequency $f = 15$ MHz is shown in Fig. 2(a). The curves were constructed at the zero-to-second mode amplitude ratio of 1:10. Figure 2(b) shows the relative variation in the SAW local wavenumber $\Delta k/k_0$ due to surface loading by a water layer as a function of the coordinate across the channel width. The maximum relative decrease in the SAW velocity on the channel axis is $\sim 0.8\%$ in this example. However, even such small changes in the velocity result in very strong transverse localization of the channel waveguide modes. For example, the localization region width W_0 for the zero mode ($1/e$ width) is given by

$$\frac{W_0}{\lambda_R} = \sqrt[4]{\frac{2N^2}{\pi^2(\Delta k/k_0)_{\max}}}, \qquad (4)$$

and is only 12.7 wavelengths in this example, that is much less than the channel width. The relative decrease in the wave field amplitude of the zero mode at the channel edge x_0 with respect to its center is given by

$$\frac{\psi(x_0)}{\psi(0)} = \exp\left[-\pi N\sqrt{\frac{1}{2}(\Delta k/k_0)_{\max}}\right]. \qquad (5)$$

At the chosen parameters, the argument of the exponent in formula (5) is -7, which means a field decrease at the edge to almost zero, i.e., almost complete localization of the zero mode within the channel. Thus, the above analysis shows that the finiteness of the microfluidic channel width can be neglected in calculating its lowest waveguide modes.

Figure 2(a) also shows the sum of the fields of the two lowest symmetric modes for the case where the amplitude of the second mode is 10% of that of the zero mode. Such a relation corresponds to the maximum amplitude of the second mode, at which no dip arises in the channel axis in the total profile, and this profile can be considered as closest to the quasirectangular distribution of exciting IDT fields. A more accurate ratio of amplitudes of various modes can be found by expanding the IDT field distribution in a series of all channel modes. However, such an expansion would require the consideration of the effect of the finite channel width on the properties of waveguide modes of higher order, and this problem is beyond the scope of this paper.

In the experiments described in [2], the liquid layer thickness arisen during drop spreading caused by SAW was comparable to the wavelength. However, this does not mean that the above analysis method is not applicable to the case studied in [2]. The point is that the necessary conditions of the applicability of the above model equation are only the closeness of region under consideration to the channel axis and the symmetry of the wave velocity profile with respect to the channel axis. Although the thin film approximation simplifies the problem, it is not necessary here. As the first of the two above mentioned conditions is satisfied, the square of the local wavenumber can be expanded in a Taylor series in powers of deviations of the layer thickness from its maximum value h_0 on the channel axis and we can restrict the analysis to the terms of the series no higher than the first order,

$$k^2(h) = k^2(h_0) + \left.\frac{\partial k^2}{\partial h}\right|_{h=h_0}\Delta h. \qquad (6)$$

Since $\Delta h = -\beta h_0 x^2$ from the second condition, we have the same functional dependence on x as that of the coefficient of the wave function in Eq. (3). The above used thin layer approximation allows us to find explicit analytical expressions for the expansion coefficients entering the right-hand side of (6). For thick layers, a more accurate approximation should be used to determine these coefficients. The dispersion relation for modes of a plane-parallel liquid layer of an arbitrary thickness, lying on an isotropic elastic halfspace, required for such calculations, is found, e.g., in [4–6],

$$\tan(Qh) = \frac{\rho_s}{\rho_{liq}}\frac{Q}{qk_t^4}D_R, \qquad (7)$$

where $D_R = 4k^2qs - (k^2 + s^2)^2$, $q = \sqrt{k^2 - k_l^2}$, $s = \sqrt{k^2 - k_t^2}$, $Q = \sqrt{k_{liq}^2 - k^2}$; $k_l = \omega/v_l$ and $k_t = \omega/v_t$ are the wavenumbers of longitudinal and transverse waves, respectively; $\omega = 2\pi f$; and ρ_s is the density of the solid halfspace. The condition $D_R = 1$ corresponds to the dispersion relation for Rayleigh waves in this halfspace. The zero mode of this system exists at any layer thickness; as the thickness varies from 0 to ∞, its phase velocity varies from the Rayleigh wave velocity v_R in the halfspace to the Stoneley wave velocity v_{St} at the interface between semi-infinite liquid and semi-infinite solid [4]. In the range of velocities from v_{liq} (the longitudinal wave velocity in liquid) to v_{St}, the trigonometrical tangent in (7) is replaced by the hyperbolic one. The critical thickness h_{cr} corresponding to this transition at $v = v_{liq}$ is determined from Eq. (7) at the tangent argument tending to zero. In this case, the replacement of the tangent by its argument yields

$$h_{cr} = \frac{\rho_s}{\rho_{liq}} \frac{D_R}{q k_t^4}, \qquad (8)$$

where D_R and q are defined at $k = k_{liq}$. From (7), an explicit exact analytical expression for the layer thickness can also be determined as a function of the wavenumber $h(k)$ or phase velocity $h(v)$ of modes. However, it is impossible to find exact inverse functional dependencies $k(h)$ and $v(h)$ in the analytical form.

In the range of velocities from v_R to v_{liq}, the discussed dependencies for the lowest mode are quite satisfactorily approximated by the expression

$$k_A^2(h) = k_R^2 + \frac{(k_{liq}^2 - k_R^2)\gamma h^4}{1 + \gamma h^4}. \qquad (9)$$

This approximation yields the result $v = v_R$ identical to the exact solution at $h = 0$. Moreover, it is identical to the exact solution at least at a single point as the velocity approaches v_{liq}. Proper selection of the coefficient γ can allow complete identity of the approximation to the exact solution at an arbitrary intermediate point v_{ip} as well. To this end, it is necessary, using the exact functional dependence $h(v)$, to find the value of h_{ip} corresponding to the chosen value of v_{ip}. Then these values of the velocity and thickness are used to find the numerical value of the coefficient γ. Figure 3 compares the exact solution to Eq. (7) (solid curves) and approximation (9) (dashed curves) for the phase velocity and its derivative with respect to the thickness for a water layer lying on the isotropic solid halfspace with the parameters $\rho_s = 4650\,\mathrm{kg\ m^{-3}}$, $v_t = 3220\,\mathrm{m\ s^{-1}}$, and $v_l = 5850\,\mathrm{m\ s^{-1}}$. The coefficient γ was calculated from the condition of the identity of the exact solution and the approximation at the point $v_{ip} = \sqrt{(v_{liq}^2 + v_R^2)/2}$. The exact solution was calculated using the explicit functional dependencies $h(v)$ and $\partial h/\partial v$ by varying the velocity v with a fixed step within a given interval. As seen in the figure, rather good agreement of not only the velocities themselves but also their derivatives is observed.

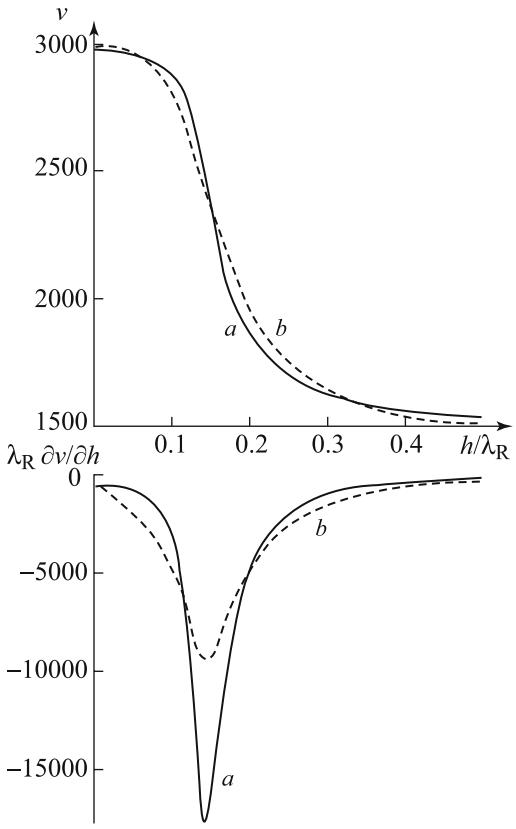

Fig. 3. Dependencies of the phase velocity v and its derivative $\partial v/\partial h$ on the relative layer thickness h/λ_R for the lowest mode in the structure consisting of the plane-parallel liquid layer on the isotropic solid halfspace: (a) the exact solution (solid curves) and (b) approximation (dashed curves).

Thus, it was shown in this study that relatively small changes in the local velocity of surface acoustic waves due to loading the surface by liquid in the region of the microfluidic channel can cause noticeable localization of the waveguide mode field near the channel axis. It is not improbable that the above studied wave localization due to a nonuniform liquid loading can also be observed in natural phenomena, e.g., during seismic Rayleigh wave propagation along riverbeds or underwater canyons in the ocean, as well as during surface sound propagation along raindrop traces on inclined or vertical solid surfaces. This study can also be of interest for analyzing the distribution of the amplitude of surface thermal (Debye) vibrations of solids. It is known that surfaces of

objects surrounding us, as a rule, are covered by thin microscopic layers of moisture adsorbed from air under ordinary atmospheric conditions. The thickness nonuniformity of such layers can cause localization of hypersonic Debye vibrations and changes in their distribution over the surface which, for quasi-one-dimensional variations in the film thickness, can be analyzed using the results of this study.

REFERENCES

1. A. Wixforth, "Acoustically Driven Planar Microfluidics," Superlatt. Microstruct. **33**(5–6), 389 (2003).
2. B. A. Korshak, V. G. Mozhaev, and A. V. Zyryanova, "Observation and Interpretation of SAW-Induced Regular and Chaotic Dynamics of Droplet Shape," in *IEEE International Ultrasonics Symposium Proceedings*, Rotterdam, 2005 (IEEE, N.Y., 2006). Vol. 2, p. 1019.
3. B. A. Auld, *Acoustic Fields and Waves in Solids* (Wiley, N.Y., 1973). Vol. 2, p. 277.
4. L. M. Brekhovskikh, *Waves in Layered Media* (Academic Press, N.Y., 1960).
5. W. M. Ewing, W. S. Jardetzky, and F. Press, *Elastic Waves in Layered Media* (McGraw-Hill, N.Y., 1957), p. 161.
6. I. A. Viktorov, *Sound Surface Waves in Solids* (Nauka, Moscow, 1981), p. 41 [in Russian].
7. I. A. Viktorov, *Rayleigh and Lamb Waves. Physical Theory and Applications* (Plenum Press, N.Y., 1967), p. 46.
8. J. K. Knowles, "A Note on Elastic Surface Waves," J. Geophys. Res. **71**(22), 5480 (1966).
9. L. A. Coldren, "Rayleigh Wave Guidance Using Anisotropic Topographic Structure," Appl. Phys. Lett. **25**(7), 367 (1974).